HHS Public Access

Author manuscript

Methods Mol Biol. Author manuscript; available in PMC 2015 April 23.

Published in final edited form as:

Methods Mol Biol. 2014 ; 1105: 419–437. doi:10.1007/978-1-62703-739-6_31.

Quantitative PCR-Based Measurement of Nuclear and Mitochondrial DNA Damage and Repair in Mammalian Cells

Amy Furda, **Janine H. Santos**, **Joel N. Meyer**, and **Bennett Van Houten**

Abstract

In this chapter, we describe a gene-specific quantitative PCR (QPCR)-based assay for the measurement of DNA damage, using amplification of long DNA targets. This assay has been used extensively to measure the integrity of both nuclear and mitochondrial genomes exposed to different genotoxins and has proven to be particularly valuable in identifying reactive oxygen species-mediated mitochondrial DNA damage. QPCR can be used to quantify both the formation of DNA damage as well as the kinetics of damage removal. One of the main strengths of the assay is that it permits monitoring the integrity of mtDNA directly from total cellular DNA without the need for isolating mitochondria or a separate step of mitochondrial DNA purification. Here we discuss advantages and limitations of using QPCR to assay DNA damage in mammalian cells. In addition, we give a detailed protocol of the QPCR assay that helps facilitate its successful deployment in any molecular biology laboratory.

Keywords

Mitochondrial DNA; Nuclear DNA; DNA damage; Reactive oxygen species (ROS); Quantitative PCR (QPCR)

1 Introduction

1.1 Principle of the Assay

The quantitative PCR (QPCR) assay of DNA damage is based on of the Assay the principle that many kinds of DNA lesions can slow down or block the progression of DNA

[10]Primers: Since the same batch of primers when used over a long period of time (several months) can give rise to lower amplification, it is valuable to make new dilutions from time to time. Always protect primer stocks from unnecessary temperature fluctuation and contamination. If frozen, primer stocks should be completely thawed prior to use (Unpublished data).

[11]dNTPs: Higher misincorporation frequency for the enzyme and reduction in effective magnesium concentration can occur if dNTPs exceed 200 μM (Unpublished data).

[12]*rTth* polymerase: Increasing amounts of the thermostable polymerase beyond 2.5 U per reaction can increase the production of nonspecific amplification products (Unpublished data).

[13]Magnesium: The optimal concentration must be determined for each set of primers and template. The *rTth* polymerase is extremely sensitive to magnesium; we advise that amplification of the fragment of interest be evaluated using varying quantities of Mg^{++}, starting from 0.9 mM and increasing by 0.1 increments (Unpublished data).

[14]Quantitative aspect of amplification—During each set of amplifications we routinely amplify a control sample in which only 50 % of the template is added to the QPCR. Depending on the DNA quality and the products being amplified, relative amplification ranging from 40 to 60 % is considered acceptable. Any experiments that are outside this range are not satisfactory, and the entire set of reactions is discarded. It may be necessary to re-optimize the PCR by varying the number of cycles to establish a linear response to increasing template concentrations from 1.25 to 30 ng (Unpublished data).

polymerase [1]. Therefore, if equal amounts of DNA from differently treated samples are QPCR-amplified under identical conditions, DNA with fewer lesions will amplify to a greater extent than more damaged DNA [2, 3]. For example, DNA from a biological sample exposed to UV radiation will be amplified less than the DNA from a corresponding untreated control sample [4]. Damage can be expressed in terms of lesions per kilobase mathematically (*see* Subheading 3.4, **step 4**) by assuming a Poisson distribution of lesions. Additionally, DNA repair kinetics can be followed by measuring restoration of amplification of the target DNA over time, after the removal of the DNA-damaging agent. QPCR can be performed using genomic DNA from cultured cells or extracted DNA from tissue obtained from treated animals (such as rat, mouse, fish, or even nematodes).

1.2 Advantages of the Assay

Strengths of QPCR include its sensitivity, the requirement for only nanogram amounts of total (genomic) DNA, its applicability to measurement of gene-specific DNA damage and repair, and the fact that it can be used to directly compare damage to nuclear DNA (nDNA) and to mitochondrial DNA (mtDNA) from the same sample. Gene-specific QPCR is highly sensitive because of the use of “long” PCR methodology that permits the quantitative amplification of fragments of genomic DNA between 10 and 25 kb in length [5, 6]. As a result, low levels of lesions (approximately 1 per 10^5 kb) can be detected, permitting the study of DNA damage and repair at levels of lesions that are biologically relevant. Because this is a PCR-based assay, it is possible to use as little as 1–2 ng of total genomic DNA, which allows analysis of a much wider range of biological samples than is feasible with other methods (such as Southern blots or HPLC electrochemical detection) that require 10–50 μg of total cellular DNA. In fact it is possible to perform this assay on one nematode that has been simply lysed in a PCR tube.

Any gene (or region of DNA) that can be specifically PCR-amplified can be studied using QPCR. Thus, it is possible to compare the rate of damage and/or repair in regions that are hypothesized to be more quickly repaired than others. For example, using this method, it was demonstrated that normal human fibroblasts showed higher rates of repair in the actively transcribed hypoxanthineguanine phosphoribosyl transferase (*HPRT*) gene than in the non-transcribed ß-globin gene (*HBB*) [4]. This study also demonstrated that repair deficiencies in cells from patients with xeroderma pigmentosum could be clearly detected with this assay. Finally, the use of genomic DNA, which includes both nuclear and mitochondrial genomes, allows direct comparison of the degree of damage and/or repair in nDNA versus mtDNA in the same biological sample. In fact, QPCR has been used successfully to quantify damage and repair in nDNA and mtDNA after many types of genotoxicants in a wide variety of cells and tissues [7–25].

1.3 Recent Discoveries Using the Gene-Specific QPCR Assay

Since the first publication of this chapter six years ago, QPCR has been utilized in a wide variety of studies. These include the utilization of the QPCR method to determine the ability of modulating experimental conditions to influence DNA damage levels or repair in mtDNA or nDNA, such as a 2009 study by Jung et al. that measured benzo[*a*]pyrene-induced DNA damage in the Atlantic killifish [26] and the 2009 Trnka et al. study showing that

MitoTEMPOL protects against the oxidative mtDNA damage caused by menadione [27] as well as many others [28–41]. QPCR has also been employed to directly compare mtDNA and nDNA damage in aged tissues [42, 43] as well as determine the effects of disease conditions [37, 44–46] and conditions such as oxidative stress [31, 40] on repair in mtDNA and nDNA. The assay has also been used to show that repair of UV photoproducts is reduced by approx 50 % in aging nematodes [47]. In addition to the range of discoveries acquired using QPCR, several recent reviews have been published regarding the adaptability of QPCR to a wide range of applications [48–50] as well as articles in which authors have adapted the QPCR technique to apply to their own field of study [26, 31, 33, 39, 51, 52].

While the importance of damage to the nuclear genome is widely recognized, the role of mtDNA damage in pathobiology and disease is only now being fully appreciated. To this end, we discuss below the consequences of damage to the mitochondrial genome.

1.4 Mitochondrial DNA Damage

The mammalian mitochondrial genome is a circular molecule present in multiple (often 2–10) copies in each mitochondrion, with hundreds to thousands of mitochondria per cell (more mitochondria are generally present in cells with high energy requirements). The human mtDNA encodes 2 rRNAs, 22 tRNAs, and 13 polypeptides, all of which are involved in oxidative phosphorylation through the electron transport chain (ETC). While the important role of nDNA damage in human pathological conditions such as cancers is well known, increasing attention is being paid to the association of mtDNA damage with various human diseases [53, 54]. Some of these include neurodegenerative disorders such as Alzheimer's, Parkinson's, and Huntington's disease [55–57]; hereditary diseases such as Leber hereditary optic neuropathy and Kearns–Sayre syndrome [58]; cancer [59]; and aging [60–62]. The MITOMAP website (http://www.mitomap.org) provides additional information and links related to mtDNA mutations and deletions and the pathological conditions associated with them.

Substantial evidence suggests that mtDNA may be more vulnerable than nDNA to certain kinds of damage, in particular reactive oxygen species (ROS)-mediated lesions [7, 14, 19]. Several reasons may underlie this observation, including the immediate proximity of mtDNA to the ETC in the inner mitochondrial membrane, which is the main source of endogenous ROS production. ROS are generated at substantial rates under normal circumstances by the ETC; it is estimated that perhaps as much as 1 % of the oxygen consumed in vitro by mitochondrial preparations is released as superoxide (O_2^-) and hydrogen peroxide (H_2O_2) [63, 64], although the in vivo level of production is probably lower [65]. The rate of ROS generation by the ETC can be increased by exposure to some xenobiotics (e.g., certain redox-cycling compounds and ETC inhibitors [62, 66]); and lipophilic xenobiotics tend to accumulate in the mitochondrial membranes (reviewed in ref. 67). Redox-active metals, such as iron and copper that can participate in Fenton chemistry, are in close proximity to or can directly bind to mtDNA [68, 69]. Additionally, mtDNA lacks many of the protective protein structures associated with nDNA, and it is believed that repair of mtDNA lesions occurs only via base excision repair [62, 70, 71]. In fact, while

oxidative damage can be repaired in the mtDNA, bulky DNA adducts, which are removed by the nucleotide excision repair machinery, are not (reviewed in ref. 67).

In the past three decades, various studies using different methodologies have identified higher rates of damage in the mtDNA than in the nDNA of the same biological sample, most notably ROS-mediated damage [7, 14, 72–74]. Early studies often relied upon DNA extraction techniques that caused extensive DNA oxidation, resulting in reports of artifactually high levels of adducts [75]. Moreover, in some cases the higher levels of damage observed in mtDNA may have been due to the additional handling necessary to first isolate mitochondria from whole-cell (or tissue) extracts in order to obtain nDNA-free mtDNA [76]. Thus, the ability of the long PCR assay to measure mtDNA damage without manipulation of mitochondria, and compare the mtDNA to nDNA damage in the same samples, makes it particularly appropriate for this use.

1.5 Limitations of the Long PCR Assay

Four limitations are associated with QPCR. First, DNA lesions that do not significantly stall progression of DNA polymerase, such as 8-hydroxydeoxyguanosine (8-OHdG), will not be detected with high efficiency by this assay. However, agents that cause oxidative stress, such as H_2O_2 or ionizing radiation, are very unlikely to produce only one type of lesion. In fact, it is estimated that only 10 % of H_2O_2-induced damage is 8-OHdG [77]. Second, although we can identify the presence of damage on the DNA template, the specific nature of the lesion cannot be inferred by QPCR alone. Both of these limitations are shared by some of the other methods available, however. An additional hypothetical concern is that, in terms of the nuclear genome, typically only one or a few genes or regions are amplified. Thus, if the nDNA damage induced by a given agent were highly regiospecific, such as for the p53 gene [78], the results of this assay could possibly be skewed (indicating no or low DNA damage if the target regions were principally away from the fragments amplified, or too many lesions if the fragments amplified were preferentially damaged). For example, it has also been shown that oxidative lesions preferentially occur at promoter regions in certain genes during aging [79]. A fourth problem has been recently encountered. Using an automated extraction method (QIAcube) that is apparently more gentle on the DNA, we have found that a large portion of mitochondrial DNA appears to exist in a supercoiled, covalently closed circular form that does not easily denature and therefore inhibits free access to primers (discussed below). Thus, mock-treated samples are not amplified as much as, for instance, H_2O_2-treated samples, whose oxidatively induced nicks and single-strand breaks convert the supercoiled mtDNA to open circular DNA, which readily denatures and increases the accessibility to primers. This inherent issue with amplification and the accurate determination of mtDNA copy number can be overcome by cutting the mtDNA with restriction enzymes that cut in regions outside of the amplified regions. For example, the *Hae*II restriction enzyme cuts the mouse mitochondrial genome in a region proximal to the D-loop that is outside the regions of amplification we use in our version of the assay. The use of restriction enzymes greatly enhances the amplification of the mtDNA in both mock-treated and treated samples, suggesting that a totally intact mitochondrial genome may inherently limit amplification (discussed below).

2 Materials (*See* Notes 1 and [2])

2.1 DNA Sample Extraction (See Note 3)

1. QIAGEN Genomic Tip (QIAGEN, Valencia, CA; cat. no. 10323).
2. QIAGEN Genomic DNA Buffer Set Kit (cat. no. 19060).

2.2 DNA Quantitation and PCR Analysis

1. Extracted DNA samples (routinely stored at −20 °C; avoid unnecessary cycles of freezing and thawing). For quantitation, dilute to a range of around 20 ng/μL. Diluted samples can be kept at 4 °C for up to several weeks before use.
2. PicoGreen dye (dsDNA quantitation reagent; Molecular Probes [Invitrogen, Carlsbad, CA], cat. no. P-7581; *see* Note 4). Store as 50 μL aliquots at −20 °C. Thaw only immediately prior to use.
3. 20× TE buffer: 200 mM Tris–HCl, 20 mM EDTA, pH 8.0. Dilute to 1×, and store at room temperature.
4. λ *Hind*III-cut DNA (Gibco [Invitrogen], cat. No. 15612-013) diluted to generate a standard curve.
5. Fluorescent plate reader with capability for measuring 485 nm excitation and 528 nm emission (e.g., Synergy 2 Multi-Mode microplate reader, BioTek, Winooski, VT).

2.3 PCR Reagents

1. GeneAmp XL PCR Kit (Perkin-Elmer, Foster City, CA) for long QPCR. Kit includes *rTth* DNA polymerase XL (400 U; 2 U/μL), 3.3× XL PCR buffer, and 25 mM Mg(OAc) 2. All reagents are stored at −20 °C.
2. Bovine serum albumin (BSA).
3. Deoxyribonucleoside triphosphates (dNTPs): Purchase separately from Pharmacia (Pfizer, New York, NY; cat. No. 27-2035-01). Prepare a solution of 10 mM total dNTPs (2.5 mM of each nucleotide) and store as 100-μL aliquots at −20 °C to

[1]In addition to high-quality reagents, the most important factor for the success of QPCR is the diligent avoidance of sample cross-contamination with PCR products. Use sterile technique for all steps. The constant use of disposable gloves when handling samples and reagents is essential to avoid the introduction of nucleases, foreign DNA, or other contaminants that can cause degradation of the template or inhibition of the polymerase during cycling.

[2]We have found that it is extremely important to have distinct, dedicated workstations for different steps of the procedure, preferably in physically separate laboratories (*see* additional information in Note 5). We also suggest that micropipettes, racks, tubes, tips, and other materials used for QPCR be exclusively used for the assay. In our laboratory, we set up PCR reactions in a hood that is sterilized with ultraviolet light (that will also extensively damage any potentially contaminating product-carryover DNA) immediately before each use.

[3]An automated method of DNA purification for QPCR has recently been developed using the QIAcube (QIAGEN, cat. no. 9001292) with the QIAamp DNA mini kit for human samples (QIAGEN, cat. no. 51304) or the DNeasy blood and tissue kit for animal samples (QIAGEN, cat. no. 69504). When using this method of extraction, the initial DNA yield is lower than when using QIAGEN Genomic tips, but the DNA endures less damage and is more homogenous. As described above (and in Fig. 3), caution must be used to accurately amplify mitochondrial DNA under these conditions.

[4]The free dye has very low fluorescence but exhibits a >1,000-fold increase in fluorescence signal upon binding to dsDNA. The assay displays a linear correlation between dsDNA quantity and fluorescence over a wide range of concentrations and is extremely sensitive (limit of detection is approximately 25 pg/mL).

minimize degradation. Thaw the dNTPs immediately prior to use, and they are reused.

4. Primer stocks and aliquots of the working concentration (10 μM) are maintained at −20 °C. The lyophilized oligos are initially diluted in sterile deionized water (to 100 μM); further dilution to the working concentration is then done with 1× TE. It is not necessary to purchase oligonucleotides purified beyond simple desalting.

3 Methods

3.1 DNA Extraction

High-molecular-weight DNA is essential in order to efficiently amplify long genomic targets. We have found that the DNA purified using the QIAGEN Genomic Tip and Genomic DNA Buffer Set Kit (QIAGEN, cat, nos. 10323 and 19060, respectively) is of high quality and quite reproducible from sample to sample. In addition, the purified DNA is very stable, yielding comparable amplification over long periods of storage.

DNA template integrity is essential for the reliable amplification of long PCR targets [80]. Although various kits are commercially available for DNA isolations, procedures that involve phenol extraction should be avoided due to potential introduction of artifactual DNA oxidation. As mentioned above, we use a DNA extraction kit from QIAGEN, which, in our hands, gives rise to templates of relatively high molecular weight and highly reproducible yield. The protocol for DNA isolation is followed as suggested by the manufacturer. Note that when using the manual genomic-tip protocol, the tissue protocol is used irrespective of whether tissue or cells are being studied, since the protocol for DNA extraction of cultured cells involves isolation of nuclei and hence loss of mtDNA. Samples that cannot be processed immediately after experiments should be stored at −80 °C until DNA is extracted. *See* additional information in Note 2.

3.2 Quantitation of DNA Template

Quantitation of the purified genomic DNA, as well as of PCR products, is performed fluorimetrically using the PicoGreen dsDNA quantitation reagent from Molecular Probes (catalog number P-7581). The free dye has very low fluorescence but exhibits a >1,000-fold increase in fluorescence signal upon binding to dsDNA. The assay displays a linear correlation between dsDNA quantity and fluorescence over a wide range of concentrations and is extremely sensitive (limit of detection is approximately 25 pg/mL).

The success of QPCR is absolutely dependent upon the accurate quantitation of the DNA present in the samples [6]. As mentioned previously, we have adopted PicoGreen as a means to quantify DNA. The DNA concentration of the samples is calculated based on a DNA standard curve, plotting the fluorescence values on a Microsoft Excel spreadsheet (*see* Fig. 1; template available upon request). Additional aspects of this procedure are found in Subheading 4.

We perform quantitation in a minimum of two different steps, called pre- and final quantitation. The first gives a rough estimate of the initial amount of DNA in each sample. At the end of this first step, the amount of DNA necessary to make a 10 ng/μL solution of

DNA is calculated. The final quantitation uses this latter solution to calculate the exact amount of DNA needed to dilute samples to 3 ng/μL, which is the amount of template routinely used for QPCR in our laboratory. Our protocol for quantitation is as follows:

1. Dilute lambda/HindIII DNA (in 1× TE buffer) yielding different concentrations to generate a standard curve (for example, from 1.25 to 20 ng/μL of DNA).
2. Add 95 μL of 1× TE buffer to each well that will be used (for standards and samples).
3. Add 5 μL of each lambda DNA standard per well (producing a curve of 0–200 ng DNA/well), at least in duplicate (*see* Note 3).
4. For pre-quantitation, pipette 5 μL of the sample DNA in duplicate at a 1:10 dilution in 1× TE.
5. Prepare a solution containing the PicoGreen reagent (5 μL reagent per mL of 1× TE). This solution is mixed, and 100 μL are added into each well containing the DNA samples.
6. Incubate for 10 min, at room temperature, in the dark (the plate can be covered with foil paper).
7. Read fluorescence; in our laboratory we use the FL600 Microplate Fluorescence Reader from Bio-Tek with the following parameters: excitation and emission wavelengths 485 and 528 nm, respectively; sensitivity limit 75; and shaking of the plate set at level 3 for 20 s. For additional details *see* Note 4.

3.3 Quantitation of PCR Products

The PicoGreen reagent has proven efficient for quantitation not only of DNA template but also of PCR products. In fact, the accuracy of the data obtained with this assay is comparable to or can exceed the reproducibility that is accomplished with ^{32}P-radiolabeled nucleotides (Chen, Y. and Van Houten, B., unpublished observation) followed by subsequent agarose gel electrophoresis. Analysis of PCR products is performed similarly to the DNA quantitation (*see* Subheading 3.2), using 10 μL of the PCR products and subtracting the fluorescence of a PCR reaction run without template. For data analysis *see* Subheading 3.4.4. *Important*: When first developing the assay in your laboratory it is essential to assess the PCR products by agarose gel electrophoresis to verify the size of the product and to assure that no other spurious products are generated.

3.4 QPCR

3.4.1 Primer Selection—The appropriate primer selection is highly important and is empirically based. In general, the oligonucleotides should be 20–24 bases in length with a G +C content of ~50 % and a T_M of ~68 °C. The selected primers should be evaluated for secondary structures using appropriate software since the formation of artifacts such as primer-dimers can compete with the QPCR reaction [6]. Additionally, the production of one unique band should be verified by gel electrophoresis prior to further use. We have purchased oligonucleotides from several vendors and find that the primers work well with no purification beyond standard desalting. Table 1 shows the sequences of the

oligonucleotides currently in use in our laboratory to amplify human, mouse, and rat target genes. *See* also Note 5.

3.4.2 PCR Reaction—Once the primers are selected, finding the optimal reaction conditions is the next step. Different target genes and different primers usually require distinct conditions. Our laboratory has established optimal concentrations of reagents to amplify specific genes of our interest. Using the Perkin-Elmer kit mentioned above, the PCR reactions are prepared as follows:

1. 15 ng of DNA (total).
2. 1× buffer.
3. 100 ng/μL final concentration of BSA.
4. 200 μM final concentration of dNTPs (*see* Note 6).
5. 20 pmol of each primer.
6. 1.3 mM final concentration of Mg^{++}.
7. Water to complete a total volume of 45 μL.

Begin the PCR reaction by a "hot start." Bring the reaction mixture to 75 °C prior to addition of enzyme (1 U/reaction, dilute 0.5 μL of the polymerase in 4.5 μL of sterile water (*see* Note 7)) and subsequent cycling.

Primers and magnesium concentrations may need to be optimized for different genes (*see* Note 8). In addition, add the reaction components to the PCR tube in a consistent order. The DNA template should be added first (remember to include a control that contains no genomic DNA—any signal produced in this sample would be indicative of a carryover problem; this is a serious problem and can only be cured by strict adherence to the conditions described above and starting with all new reagents), followed by the PCR mix, and finally the enzyme (as a hot start). In our laboratory reactions are set up at room temperature.

3.4.3 Cycle Number Parameters and Thermal—The usefulness of the QPCR assay for the detection of DNA damage requires that amplification yields be directly proportional to the starting amount of template. These conditions must be met by keeping the PCR in the exponential phase. The first step towards this criterion is to perform cycle tests to determine quantitative conditions for the gene of interest [3]. This can be accomplished using a non-

[5]Because of the long run time of our PCR programs, we add BSA (100 ng/μL final concentration) to the PCR mix to increase the stability of the polymerase [6].

[6]It is of extreme importance not to open the PCR tubes after the last cycle in the same laboratory where the reactions were set up. Small DNA quantities can volatilize and contaminate other reactions, particularly if the tube is still hot, and completed reactions contain very high numbers of PCR products. The inclusion of a blank sample (where no DNA is added) helps to assure that no contamination has occurred with spurious DNA or PCR products. This sample should give no DNA band, if checked on gel, nor high fluorescence signal (as gauged by PicoGreen).

[7]When extracting DNA, vortex the samples well prior to lysis and again before adding them to the columns. This vortexing does not affect the subsequent amplification of the DNA.

[8]Load samples as well as standard DNA in duplicates, and average the fluorescent reading of two wells. This helps increase the accuracy of the readings and, thus, of the estimated concentration.

damaged sample and a “50 % control” containing half of the amount of the non-damaged template (1.5 ng/μL DNA). This control should give a 50 % reduction of the amplification signal (*see* Note 9). Thus, a cycle test should identify a range of cycles over which the product amplification is exponential and 50 % controls are very close to 50 %. Once the optimal number of cycles is identified, always run this 50 % control as a quality control.

Another concern when performing QPCR is finding the optimal thermal conditions for amplification of your target gene. As mentioned before, QPCR in our laboratory is routinely performed using hot start, which produces cleaner PCR products because it prevents nonspecific annealing of primers to each other, as well as to template, before enzyme addition. Keep in mind that the melting temperature of the primers and the annealing temperature used in the PCR determine how stably and specifically the primers hybridize to the DNA template. Thus, it is important to check this parameter with suitable software beforehand, and annealing temperatures must be experimentally optimized. Table 2 shows the most favorable conditions for human and rodent amplifications currently used in our laboratory.

3.4.4 Data Analysis—Analysis of data obtained by the PicoGreen protocol described above is done using a Microsoft Excel spreadsheet (*see* example in Fig. 2). The fluorescence readings (of the duplicated samples) are averaged, and blank value (from no-DNA control) is subtracted. These values are used to calculate the “relative amplification,” which refers to the comparison between amplification of treated samples with non-treated (or undamaged) control. This is accomplished simply by dividing the respective fluorescence values. These results are then used to determine the lesion frequency per fragment at a particular dose, such that lesions/strand (average for both strands) at dose $D=-\ln A_D/A_C$. This equation is based on the “zero class” of a Poisson expression. Note that a Poisson distribution requires an assumption that DNA lesions are randomly distributed. We normally analyze each DNA sample in two separate PCR runs which allows higher reproducibility.

3.4.5 Normalization to mtDNA Copy Number—It is known that DNA content can vary in mitochondria from different cells or tissues, depending, for instance, on energy requirements. Thus, in samples from distinct areas of a specific organ, one could expect discrepancies in the ability to amplify the mtDNA based not on different levels of lesions within the sample but simply from fluctuation in the number of copies of the mitochondrial genome present. Therefore, to normalize for mitochondrial copy number, we routinely amplify an additional short fragment (no longer than 300 bp) of the mitochondrial gene under study. The idea is that the amplification of the short fragment reflects only undamaged DNA due to the low probability of introducing lesions in small segments. The results obtained with the short sequence are used to monitor the copy number of the mitochondrial genome and, more importantly, to normalize the data obtained with the large (7–15 kb) fragment. As noted above if DNA is extracted using an automated system employing the QIAcube (QIAGEN, catalog number 9001292) with the QIAamp DNA mini kit for human

[9]Make sure that the samples are well homogenized (by vortexing, for example) prior to quantitation. If samples are still highly concentrated after the first dilution (i.e., well above 10 ng/μL), we recommend an additional round of quantitation. This assures accuracy of the concentration of the final 3 ng/μL solution.

samples (QIAGEN, catalog number 51304), linearization of the mtDNA is necessary to get an accurate level of mtDNA. We have found that HaeII is compatible with our primer sets for mouse mtDNA (*see* Fig. 3) and *Pvu*II or *Cla*I are compatible with our primer sets for human mtDNA.

References

1. Ponti M, Forrow SM, Souhami RL, D'Incalci M, Hartley JA. Measurement of the sequence specificity of covalent DNA modification by antineoplastic agents using *Taq* DNA polymerase. Nucleic Acids Res. 1991; 19:2929–2933. [PubMed: 2057351]
2. Jennerwein MM, Eastman A. A polymerase chain reaction-based method to detect cisplatin adducts in specific genes. Nucleic Acids Res. 1991; 19:6209–6214. [PubMed: 1956780]
3. Kalinowski DP, Illenye S, Van Houten B. Analysis of DNA damage and repair in murine leukemia L1210 cells using a quantitative polymerase chain reaction assay. Nucleic Acids Res. 1992; 20:3485–3494. [PubMed: 1630919]
4. Van Houten B, Cheng S, Chen Y. Measuring DNA damage and repair in human genes using quantitative amplification of long targets from nanogram quantities of DNA. Mutat Res. 2000; 460:81–94. [PubMed: 10882849]
5. Van Houten B, Chen Y, Nicklas JA, Rainville IR, O'Neill JP. Development of long PCR techniques to analyze deletion mutations of the human hprt gene. Mutat Res. 1998; 403:171–175. [PubMed: 9726017]
6. Ayala-Torres S, Chen Y, Svoboda T, Rosenblatt J, Van Houten B. Analysis of gene- specific DNA damage and repair using quantitative polymerase chain reaction. Methods. 2000; 22:135–147. [PubMed: 11020328]
7. Yakes FM, Van Houten B. Mitochondrial DNA damage is more extensive and persists longer than nuclear DNA damage in human cells following oxidative stress. Proc Natl Acad Sci U S A. 1997; 94:514–519. [PubMed: 9012815]
8. Mandavilli BS, Ali SF, Van Houten B. DNA damage in brain mitochondria caused by aging and MPTP treatment. Brain Res. 2000; 885:45–52. [PubMed: 11121528]
9. Moon SK, Thompson LJ, Madamanchi N, et al. Aging, oxidative responses, and prolif-erative capacity in cultured mouse aortic smooth muscle cells. Am J Physiol Heart Circ Physiol. 2001; 280:H2779–H2788. [PubMed: 11356636]
10. Denissenko MF, Cahill J, Koudriakova TB, Gerber N, Pfeifer GP. Quantitation and mapping of aflatoxin B1-induced DNA damage in genomic DNA using aflatoxin B1-8,9-epoxide and microsomal activation systems. Mutat Res. 1999; 425:205–211. [PubMed: 10216213]
11. Ballinger SW, Patterson C, Knight-Lozano CA, et al. Mitochondrial integrity and function in atherogenesis. Circulation. 2002; 106:544–549. [PubMed: 12147534]
12. Jin GF, Hurst JS, Godley BF. Rod outer segments mediate mitochondrial DNA damage and apoptosis in human retinal pigment epithelium. Curr Eye Res. 2001; 23:11–19. [PubMed: 11821981]
13. Sawyer DE, Mercer BG, Wiklendt AM, Aitken RJ. Quantitative analysis of gene- specific DNA damage in human spermatozoa. Mutat Res. 2003; 529:21–34. [PubMed: 12943917]
14. Santos JH, Hunakova L, Chen Y, Bortner C, Van Houten B. Cell sorting experiments link persistent mitochondrial DNA damage with loss of mitochondrial membrane potential and apop-totic cell death. J Biol Chem. 2003; 278:1728–1734. [PubMed: 12424245]
15. Yanez JA, Teng XW, Roupe KA, Fariss MW, Davies NM. Chemotherapy induced gastrointestinal toxicity in rats: involvement of mitochondrial DNA, gastrointestinal permeability and cyclooxygenase-2. J Pharmacol Pharmaceut Sci. 2003; 6:308–314.
16. O'Brien T, Xu J, Patierno SR. Effects of glutathione on chromium-induced DNA cross-linking and DNA polymerase arrest. Mol Cell Biochem. 2001; 222:173–182. [PubMed: 11678599]
17. Chandrasekhar D, Van Houten B. High resolution mapping of UV-induced photo-products in the *Escherichia coli lacI* gene: Inefficient repair of the non-transcribed strand correlates with high mutation frequency. J Mol Biol. 1994; 238:319–332. [PubMed: 8176728]

18. Yakes, FM.; Chen, Y.; Van Houten, B. PCR-based assays for the detection and quantitation of DNA damage and repair. In: Pfeifer, GP., editor. Technologies for detection of DNA damage and mutations. Plenum Press; New York, NY: 1996. p. 171-184.
19. Salazar JJ, Van Houten B. Preferential mitochondrial DNA injury caused by glucose oxidase as a steady generator of hydrogen peroxide in human fibroblasts. Mutat Res. 1997; 385:139–149. [PubMed: 9447235]
20. Chen KH, Yakes FM, Srivastava DK, et al. Up-regulation of base excision repair correlates with enhanced protection against a DNA damaging agent in mouse cell lines. Nucleic Acids Res. 1998; 26:2001–2007. [PubMed: 9518496]
21. Horton JK, Roy G, Piper JT, et al. Characterization of a chlorambucil-resistant human ovarian carcinoma cell line overexpressing glutathione S-transferase μ. Biochem Pharmacol. 1999; 58:693–702. [PubMed: 10413308]
22. Deng G, Su JH, Ivins KJ, Van Houten B, Cotman CW. Bcl-2 facilitates recovery from DNA damage after oxidative stress. Exptl Neurol. 1999; 159:309–318. [PubMed: 10486199]
23. Ballinger SW, Patterson C, Yan CN, et al. Hydrogen peroxide- and peroxynitrite-induced mitochondrial DNA damage and dysfunction in vascular endothelial and smooth muscle cells. Circ Res. 2000; 86:960–966. [PubMed: 10807868]
24. Chandrasekhar D, Van Houten B. In vivo formation and repair of cyclobutane pyrimidine dimers and 6–4 photoproducts measured at the gene and nucleotide level in *Escherichia coli*. Mutat Res. 2000; 450:19–40. [PubMed: 10838132]
25. Sobol RW, Watson DE, Nakamura J, et al. Mutations associated with base excision repair deficiency and methylation-induced genotoxic stress. Proc Natl Acad Sci U S A. 2002; 99:6860–6865. [PubMed: 11983862]
26. Jung D, Cho Y, Collins LB, Swenberg JA, Di Giulio RT. Effects of benzo[*a*]pyrene on mitochondrial and nuclear DNA damage in Atlantic killifish (*Fundulus heteroclitus*) from a creosote-contaminated and reference site. Aquat Toxicol. 2009; 95:44–51. [PubMed: 19726093]
27. Trnka J, Blaikie FH, Logan A, Smith RA, Murphy MP. Antioxidant properties of MitoTEMPOL and its hydroxylamine. Free Radic Res. 2009; 43:4–12. [PubMed: 19058062]
28. Lu B, Yadav S, Shah PG, et al. Roles for the human ATP-dependent Lon protease in mitochondrial DNA maintenance. J Biol Chem. 282:17363–17374. [PubMed: 17420247]
29. Ahmed S, Passos JF, Birket MJ, et al. Telomerase does not counteract telomere shortening but protects mitochondrial function under oxidative stress. J Cell Sci. 2008; 121:1046–1053. [PubMed: 18334557]
30. Rothfuss O, Fischer H, Hasegawa T, et al. Parkin protects mitochondrial genome integrity and supports mitochondrial DNA repair. Hum Mol Genet. 2009; 18:3832–3850. [PubMed: 19617636]
31. Chatterjee A, Mambo E, Zhang Y, Deweese T, Sidransky D. Targeting of mutant *hogg1* in mammalian mitochondria and nucleus: effect on cellular survival upon oxidative stress. BMC Cancer. 2006; 6:235. [PubMed: 17018150]
32. Maloney SC, Adair JE, Smerdon MJ, Reeves R. Gene-specific nucleotide excision repair is impaired in human cells expressing elevated levels of high mobility group A1 nonhistone proteins. DNA Repair. 2007; 6:1371–1379. [PubMed: 17540622]
33. Boyd WA, Crocker TL, Rodriguez AM, et al. Nucleotide excision repair genes are expressed at low levels and are not detectably inducible in *Caenorhabditis elegans* somatic tissues, but their function is required for normal adult life after UVC exposure. Mutat Res. 2010; 683:57–67. [PubMed: 19879883]
34. Ma W, Panduri V, Sterling JF, Van Houten B, Gordenin DA, Resnick MA. The transition of closely opposed lesions to double-strand breaks during long-patch base excision repair is prevented by the coordinated action of DNA polymerase ∂ and Rad27/Fen1. Mol Cell Biol. 2009; 29:1212–1221. [PubMed: 19075004]
35. Liu P, Qian L, Sung JS, et al. Removal of oxidative DNA damage via FEN1-dependent long-patch base excision repair in human cell mitochondria. Mol Cell Biol. 2008; 28:4975–4987. [PubMed: 18541666]
36. Salmon AB, Ljungman M, Miller RA. Cells from long-lived mutant mice exhibit enhanced repair of ultraviolet lesions. J Gerontol A Biol Sci Med Sci. 2008; 63:219–231. [PubMed: 18375871]

37. Acevedo-Torres K, Berrios L, Rosario N, et al. Mitochondrial DNA damage is a hallmark of chemically induced and the R6/2 transgenic model of Huntington's disease. DNA Repair. 2009; 8:126–136. [PubMed: 18935984]
38. Mao L, Wertzler KJ, Maloney SC, Wang Z, Magnuson NS, Reeves R. HMGA1 levels influence mitochondrial function and mitochondrial DNA repair efficiency. Mol Cell Biol. 2009; 29:5426–5440. [PubMed: 19687300]
39. Jung D, Cho Y, Meyer JN, Di Giulio RT. The long amplicon quantitative PCR for DNA damage assay as a sensitive method of assessing DNA damage in the environmental model, Atlantic killifish (*Fundulus heteroclitus*). Comp Biochem Physiol C Toxicol Pharmacol. 2009; 149:182–186. [PubMed: 18706522]
40. Duxin JP, Dao B, Martinsson P, et al. Human Dna2 is a nuclear and mitochondrial DNA maintenance protein. Mol Cell Biol. 2009; 29:4274–4282. [PubMed: 19487465]
41. Acevedo-Torres K, Fonseca-Williams S, Ayala-Torres S, Torres-Ramos CA. Requirement of the *Saccharomyces cerevisiae APN1* gene for the repair of mitochondrial DNA alkylation damage. Environ Mol Mutagen. 2009; 50:317–327. [PubMed: 19197988]
42. Wang AL, Lukas TJ, Yuan M, Du N, Tso MO, Neufeld AH. Autophagy and exosomes in the aged retinal pigment epithelium: possible relevance to drusen formation and age- related macular degeneration. PLoS One. 2009; 4:e4160. [PubMed: 19129916]
43. Wang AL, Lukas TJ, Yuan M, Neufeld AH. Increased mitochondrial DNA damage and down-regulation of DNA repair enzymes in aged rodent retinal pigment epithelium and choroid. Mol Vis. 2008; 14:644–651. [PubMed: 18392142]
44. Bonner M, Kmiec EB. DNA breakage associated with targeted gene alteration directed by DNA oligonucleotides. Mutat Res. 2009; 669:85–94. [PubMed: 19463835]
45. Khurana RN, Parikh JG, Saraswathy S, Wu GS, Rao NA. Mitochondrial oxidative DNA damage in experimental autoimmune uveitis. Invest Ophthalmol Vis Sci. 2008; 49:3299–3304. [PubMed: 18450595]
46. Haugen AC, Di Prospero NA, Parker JS, et al. Altered gene expression and DNA damage in peripheral blood cells from Friedreich's ataxia patients: cellular model of pathology. PLoS Genet. 2010; 6:e1000812. [PubMed: 20090835]
47. Meyer JN, Boyd WA, Azzam GA, Haugen AC, Freedman JH, Van Houten B. Decline of nucleotide excision repair capacity in aging *Caenorhabditis elegans*. Genome Biol. 2007; 8:R70. [PubMed: 17472752]
48. Meyer JN. QPCR: a tool for analysis of mitochondrial and nuclear DNA damage in ecotoxicology. Ecotoxicology. 2010; 19:804–811. [PubMed: 20049526]
49. Hunter SE, Jung D, Di Giulio RT, Meyer JN. The QPCR assay for analysis of mitochondrial DNA damage, repair, and relative copy number. Methods. 2010; 51:444–451. [PubMed: 20123023]
50. Kovalenko OA, Santos JH. Analysis of oxidative damage by gene-specific quantitative PCR. Curr Protoc Hum Genet. 2009; 62:19.1.1–19.1.13.
51. Song GJ, Lewis V. Mitochondrial DNA integrity and copy number in sperm from infertile men. Fertil Steril. 2008; 90:2238–2244. [PubMed: 18249386]
52. Edwards JG. Quantification of mitochondrial DNA (mtDNA) damage and error rates by real-time QPCR. Mitochondrion. 2009; 9:31–35. [PubMed: 19105983]
53. Wallace DC. Mitochondrial diseases in man and mouse. Science. 1999; 283:1482–1488. [PubMed: 10066162]
54. DiMauro S, Schon EA. Mitochondrial DNA mutations in human disease. Am J Med Genet. 2001; 106:18–26. [PubMed: 11579421]
55. Wallace DC, Shoffner JM, Trounce I, et al. Mitochondrial DNA mutations in human degenerative diseases and aging. Biochim Biophys Acta. 1995; 1271:141–151. [PubMed: 7599200]
56. Bowling AC, Beal MF. Bioenergetic and oxidative stress in neurodegenerative diseases. Life Sci. 1995; 56:1151–1171. [PubMed: 7475893]
57. Schapira AH. Mitochondrial dysfunction in neurodegenerative disorders. Biochim Biophys Acta. 1998; 1366:225–233. [PubMed: 9714816]
58. Wallace DC. Mitochondrial DNA mutations in diseases of energy metabolism. J Bioenerg Biomembr. 1994; 26:241–250. [PubMed: 8077179]

59. Penta JS, Johnson FM, Wachsman JT, Copeland WC. Mitochondrial DNA in human malignancy. Mutat Res. 2001; 488:119–133. [PubMed: 11344040]
60. Cadenas E, Davies KJ. Mitochondrial free radical generation, oxidative stress, and aging. Free Radic Biol Med. 2000; 29:222–230. [PubMed: 11035250]
61. Hudson EK, Hogue BA, Souza-Pinto NC, et al. Age-associated change in mitochondrial DNA damage. Free Radic Res. 1998; 29:573–579. [PubMed: 10098461]
62. Mandavilli BS, Santos JH, Van Houten B. Mitochondrial DNA repair and aging. Mutat Res. 2002; 509:127–151. [PubMed: 12427535]
63. Boveris, A.; Cadenas, E. Superoxide and hydrogen peroxide in mitochondria. In: Pryor, WA., editor. Free radicals in biology. Academic; San Diego, CA: 1982. p. 65-90.
64. Turrens JF, Boveris A. Generation of superoxide anion by the NADH dehydroge-nase of bovine heart mitochondria. Biochem J. 1980; 191:421–427. [PubMed: 6263247]
65. Beckman KB, Ames BN. Endogenous oxidative damage of mtDNA. Mutat Res. 1999; 424:51–58. [PubMed: 10064849]
66. Kowaltowski AJ, Vercesi AE. Mitochondrial damage induced by conditions of oxidative stress. Free Radic Biol Med. 1999; 26:463–471. [PubMed: 9895239]
67. Sawyer DE, Van Houten B. Repair of DNA damage in mitochondria. Mutat Res. 1999; 434:161–176. [PubMed: 10486590]
68. Massa EM, Giulivi C. Alkoxyl and methyl radical formation during cleavage of tert-butyl hydroperoxide by a mitochondrial membrane-bound, redox active copper pool: an EPR study. Free Radic Biol Med. 1993; 14:559–565. [PubMed: 8394271]
69. Walter, PB.; Beckman, KB.; Ames, BN. The role of iron and mitochondria in aging. In: Cadenas, E.; Packers, L., editors. Understanding the process of aging: the roles of mitochondria, free radicals, and antioxidants. Marcel Dekker; New York, NY: 1999. p. 203-227.
70. Croteau DL, Stierum RH, Bohr VA. Mitochondrial DNA repair pathways. Mutat Res. 1999; 434:137–148. [PubMed: 10486588]
71. Bohr VA. Repair of oxidative DNA damage in nuclear and mitochondrial DNA, and some changes with aging in mammalian cells. Free Radic Biol Med. 2002; 32:804–812. [PubMed: 11978482]
72. Mecocci P, MacGarvey U, Beal MF. Oxidative damage to mitochondrial DNA is increased in Alzheimer's disease. Ann Neurol. 1994; 36:747–751. [PubMed: 7979220]
73. Mecocci P, MacGarvey U, Kaufman AE, Koontz D, Shoffner JM, Wallace DC, et al. Oxidative damage to mitochondrial DNA shows marked age-dependent increases in human brain. Ann Neurol. 1993; 34(4):609–616. [PubMed: 8215249]
74. Zastawny TH, Dabrowska M, Jaskolski T, et al. Comparison of oxidative base damage in mitochondrial and nuclear DNA. Free Radic Biol Med. 1998; 24:722–725. [PubMed: 9586801]
75. Helbock HJ, Beckman KB, Shigenaga MK, et al. DNA oxidation matters: the HPLC-electrochemical detection assay of 8-oxo-deoxyguanosine and 8-oxo-guanine. Proc Natl Acad Sci U S A. 1998; 95:288–293. [PubMed: 9419368]
76. Anson RM, Hudson E, Bohr VA. Mitochondrial endogenous oxidative damage has been overestimated. FASEB J. 2000; 14:355–360. [PubMed: 10657991]
77. Termini J. Hydroperoxide-induced DNA damage and mutations. Mutat Res. 2000; 450:107–124. [PubMed: 10838137]
78. Quan T, States JC. Preferential DNA damage in the *p53* gene by benzo[a]pyrene metabolites in cytochrome P4501A1-expressing xeroderma pigmentosum group A cells. Mol Carcinog. 1996; 16:32–43. [PubMed: 8634092]
79. Lu T, Pan Y, Kao SY, et al. Gene regulation and DNA damage in the ageing human brain. Nature. 2004; 429:883–891. [PubMed: 15190254]
80. Cheng S, Chen Y, Monforte JA, Higuchi R, Van Houten B. Template integrity is essential for PCR amplification of 20- to 30-kb sequences from genomic DNA. PCR Methods Appl. 1995; 4:294–298. [PubMed: 7580917]

Pre Quant

Standard

Standard (ng/µL)	*read 1*	*read 2*	*mean*
0	281	265	273
1.25	20272	20195	20233.5
2.5	27329	26594	26961.5
5	80817	78756	79786.5
10	143198	140638	141918
20	386748	393562	390155

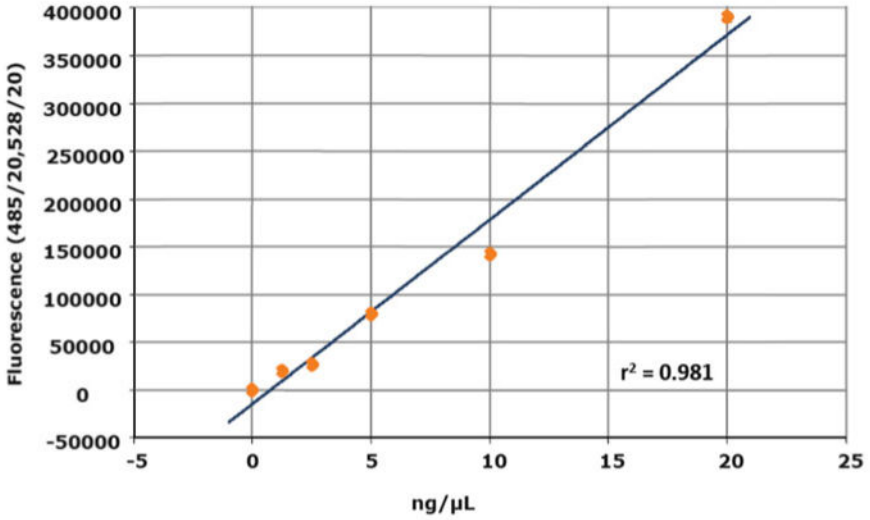

DNA samples **200 µL at 3 ng/µL**

DNA sample	Read 1	Read 2	mean	Conc (ng/µL)	DNA (µL)	TE (µL)
1	50721	50188	50454.5	3.38	177.5	22.5
2	69751	71752	70751.5	4.431	135.4	64.6
3	52235	51916	52075.5	3.464	173.2	26.8
4	61328	62739	62033.5	3.98	150.8	49.2

Fig. 1.

(**a**) Spreadsheet used for DNA quantitation. Example depicts fluorescence values obtained during the first step of quantitation, pre-quantitation, and the graph shows values obtained for the standard curve. Above the graph are all calculations related to the DNA standard curve. The first column represents the concentrations of DNA used as standards. The second and third columns show the raw fluorescence readings. These values were averaged (last column). Below the graph is an example of values obtained for an experimental set of DNA samples. Read 1 and Read 2 columns show raw fluorescence readings for each sample; the third column is the mean of those values. DNA concentration is calculated based on the slope of the standard curve. The last two columns show, respectively, the amount of DNA and of TE buffer necessary to dilute the sample DNA to 3 ng/µL

Samples	Read 1	Read 2	Mean	Final Read	Rel. Amp.	Lesions	Lesions/10Kb
50%	3012	3015	3013.5	1973	*0.53*		
control	4685	4877	4781	3740.5	*1.00*		
5'	3609	3545	3577	2536.5	*0.68*	0.388	***0.436442825***
15'	2875	2985	2930	1889.5	*0.51*	0.683	***0.76731129***
30'	1370	1382	1376	335.5	*0.09*	2.411	***2.709384961***
60'	1321	1373	1347	306.5	*0.08*	2.502	***2.810962715***
blank	1028	1053	1040.5	0			

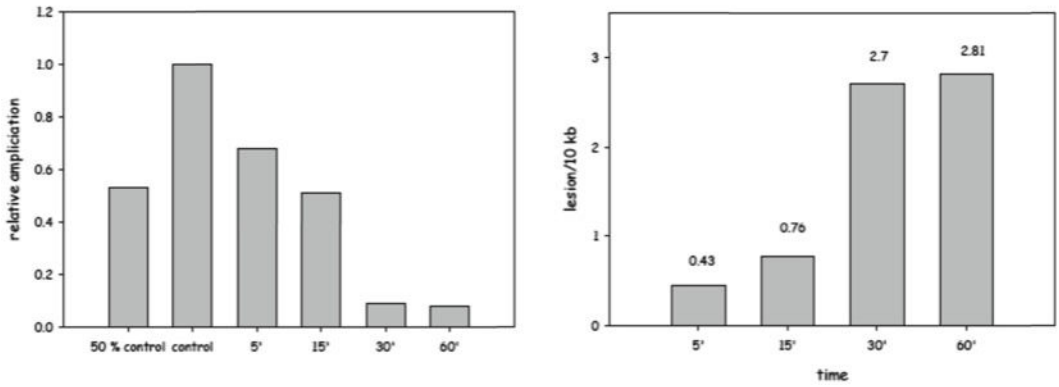

Fig. 2.

Representation of the raw fluorescence values obtained after PCR amplification of the mitochondrial genome of mammalian fibroblasts exposed to 200 μM of hydrogen peroxide for the indicated times. Column one, sample identification; columns two and three, raw fluorescence readings for each sample; fourth column, average of values from first two columns; these values are then background corrected (column 5). Relative amplification (column 6) is calculated comparing the values of the treated samples with undamaged control and is plotted in the *left* graph. Lesion frequency (column 7) is obtained based on the values plotted on column 6 and are expressed as lesions per 10 kb of the mitochondrial genome (column 8 and *right* graph)

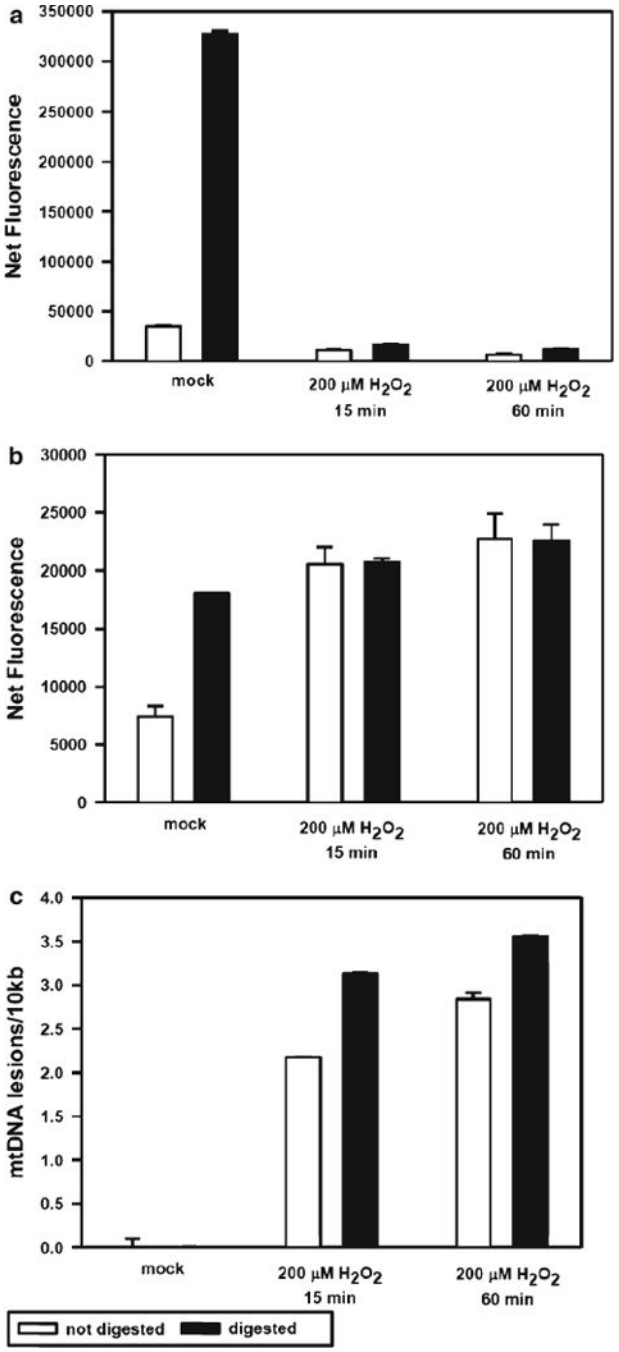

Fig. 3.

PCR products of QIAcube-extracted mouse DNA+/−digestion with HaeII. QIAcube extraction apparently results in mostly covalently closed supercoiled mtDNA, which limits primer access. HaeII digestion near the D-Loop (bp ~2,607) greatly increases amplification of the large target. Raw fluorescence values of Lmito (**a**) and Smito (**b**) and hence lesion frequencies (**c**) are affected by digestion. Lesion frequencies represent the decrease in amplification of the large mitochondrial fragment normalized to the small fragment. Data

represent the mean+/−SD of two biological samples. Net fluorescence: Picogreen fluorescence of the PCR product minus a “no-template” control

Table 1

Gene targets and primer pairs for QPCR

Human primers		
8.9 kb mitochondria fragment, accession number J01415		
14841	5′-TTT CAT CAT GCG GAG ATG TTG GAT GG-3′	Sense
5999	5′-TCT AAG CCT CCT TAT TCG AGC CGA-3′	Antisense
12.2 kb region of the DNA polymerase beta gene, accession number L11607		
2372	5′-CAT GTC ACC ACT GGA CTC TGC AC-3′	Sense
3927	5′-CCT GGA GTA GGA ACA AAA ATT GCT G-3′	Antisense
Mouse primers		
6.6 kb fragment of the DNA polymerase beta gene, accession number AA79582		
Chr8, 23735019	5′-TAT CTC TCT TCC TCT TCA CTT CTC CCC TGG-3′	Sense
Chr8, 23741702	5′-CGT GAT GCC GCC GTT GAG GGT CTC CTG-3′	Antisense
10 kb mitochondria fragment		
3278	5′-GCC AGC CTG ACC CAT AGC CAT AAT AT-3′	Sense
13337	5′-GAG AGA TTT TAT GGG TGT AAT GCG G-3′	Antisense
117 bp mitochondria fragment		
13597	5′-CCC AGC TAC TAC CAT CAT TCA AGT-3′	Sense
13688	5′-GAT GGT TTG GGA GAT TGG TTG ATG T-3′	Antisense
Rat primers		
12.5 kb fragment from the clusterin (TRPM-2) gene, accession number M64733		
5781	5′-AGA CGG GTG AGA CAG CTG CAC CTT TTC-3′	Sense
18314	5′-CGA GAG CAT CAA GTG CAG GCA TTA GAG-3′	Antisense
13.4 kb mitochondria fragment		
13559	5′-AAA ATC CCC GCA AAC AAT GAC CAC CC-3′	Sense
10633	5′-GGC AAT TAA GAG TGG GAT GGT CGG TT-3′	Antisense
211 bp mitochondria fragment		
14678	5′-CCT CCC ATT CAT TAT CGC CGC CCT TGC-3′	Sense
14885	5′-GTC TGG GTC TCC TAG TAG GTC TGG GAA-3′	Antisense

Table 2

PCR conditions for human and rodent targets

Target	Primer set	Mg++ conc. (mM)	T_M (°C)	Cycle number
Human				
Large mito	5999/14841	1.2	64	19
Small mito	14620/14841	1.1	60	19
β-pol	3927/2372	1.2	64	26
Mouse				
Large mito	3278/13337	1.2	64	19
Small mito	13688/13597	1.1	60	19
β-pol	MBFor1/MBEX1B	1.2	64	26
Rat				
Large mito	10633/13559	1.2	65	20
Small mito	14678/14885	1.1	60	20
Clusterin	5781/18314	1.2	65	28